

## **A Method of Obtaining Skin Color Distribution Areas Based on Illumination Compensation**

Sang-Hong Lee<sup>1</sup>, Seok-Woo Jang\*<sup>2</sup>

<sup>1</sup>Professor, Department of Computer Engineering, Anyang University, 22, 37-Beongil, Samdeok-Ro, Manan-Gu, Anyang 14028, Republic of Korea

\*<sup>2</sup>Professor, Department of Software, Anyang University, 22, 37-Beongil, Samdeok-Ro, Manan-Gu, Anyang 14028, Republic of Korea

shleedosa@anyang.ac.kr<sup>1</sup>, swjang7285@gmail.com\*<sup>2</sup>

Corresponding author\* : mobile Phone: +82-10-9482-6547

### **Abstract**

**Background/Objectives:** The ultra-high-speed camera captures even the slightest changes in ambient lighting as an image. Therefore, research is needed to correct the effect of lighting that is non-uniformly included in the image.

**Methods/Statistical analysis:** This paper proposes an algorithm that corrects irregular lighting from high-speed color images continuously input with a slight time interval, and then obtains an exposed skin region, which is a region of interest, from the corrected image. In this study, the non-uniform lighting effect is first corrected using a frame blending technique. Then, a region of interest is obtained from the image by applying an elliptical skin model.

**Findings:** Experimental results show that the proposed approach corrects the illumination from the input image and then accurately acquires the region of interest. In this study, the performance of the proposed method of acquiring skin pixels using illumination correction of images input at high speed was quantitatively compared and measured in terms of accuracy. In this study, a measure described as the relative ratio between the number of skin regions correctly acquired in the received images and the number of skin regions originally included in all images was used. In the conventional approach, the process of correcting irregular lighting in images was not normally performed. In addition, since a fixedly generated skin color distribution model is used, it is difficult to accurately extract skin pixels. On the other hand, the algorithm proposed in this paper effectively corrects the uneven lighting effect reflected in the image through frame blending between successive images, and then acquires the region of interest, allowing it to obtain skin color regions more robustly than conventional approaches.

**Improvements/Applications:** The proposed algorithm is expected to be useful in various kinds of practical application programs related to image recognition such as face recognition, lighting correction and removal, video indexing, etc.

**Keywords:** Image data, Illumination condition, Weight factor, Performance evaluation, Skin region.

## 1. Introduction

With the development of high-performance and small-sized image capture sensors, ultra-high-speed cameras, which are relatively inexpensive, have begun to spread [1]. Accordingly, smartphones and digital camera camcorders have begun to be equipped with functions that support semi-high-speed shooting. Such a high-speed camera can be very useful for object recognition and modeling in various practical application fields that perform image processing [2-4].

In general, ultra-high-speed cameras can shoot hundreds to thousands of frames per second. In other words, even scenes that are difficult to discern with the human eye can be detected even a minute movement of the scene when photographed with a high-speed camera. On the other hand, a high-speed camera also has a disadvantage that it may cause difficulty in image processing because it captures even too small changes in ambient lighting as an image.

Therefore, a study is needed to correctly compensate for the effects of lighting irregularly or non-uniformly included in the ultra-high-speed color image that is continuously photographed at a high speed under general indoor and outdoor environmental conditions, and to robustly acquire major areas of interest [5] such as human skin color distribution areas from light-corrected ultra-fast images.

Existing studies conducted to compensate for the lighting effects present in the image from the color image data taken or to obtain areas of interest can be found in relevant references. The method described in the study [6] proposes a lighting recovery model that converts severely changing lighting into weaker lighting. In the study [7], inspired by the visual adaptation system of the human retina, they proposed a lighting adjustment mechanism that mimics retinal processing to reduce changes in lighting. In the study [8], the effect of the lighting normalization technique to reduce the deformation caused by makeup in the face recognition system was studied. In the study [9], a very simple deep learning-based image lighting correction architecture that operates on the color image of a picture is presented regardless of whether the lighting is insufficient or excessively illuminated. In addition to the above-described approach, algorithms for correcting illumination in an image or accurately acquiring a region of interest are continuously emerging [10].

However, the existing methods described previously mainly target general flat-speed images, but not high-speed images. Therefore, the existing methods still have problems and drawbacks for various environmental changes that exist in methods for targeting flat-speed images. In addition, since research on ultra-high-speed image processing has just begun in earnest, there are many issues to be resolved.

Therefore, in this paper, we propose a technique to effectively correct illumination using a frame blending technique from the color image continuously input with a slight time interval, and then accurately acquire human skin regions, which are of interest, from images whose illumination is corrected with an elliptical color distribution model. Fig. 1 shows an overview of the approach to acquiring a region of interest using illumination correction in continuous images presented in this paper.

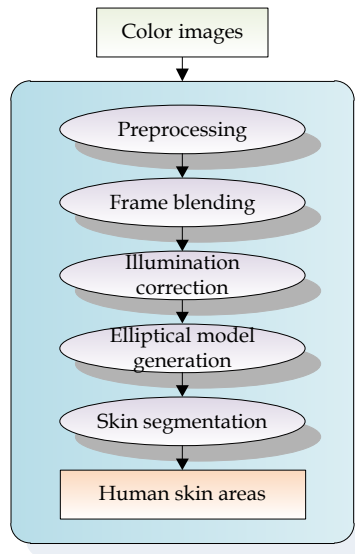


**Figure 1. Overall flow of the suggested approach**

As can be seen in Fig. 1, the technique introduced in this paper first corrects the lighting effects that are irregularly present in the image through frame blending from continuously input color images. A region of interest, which is a skin color region representing the exposed personal information of a person, is then obtained from the color image corrected for illumination.

In Chapter 1, the general introduction and outline of this study were explained. Chapter 2 describes a technique for correcting lighting using frame blending from a received color image. In Chapter 3, a method of acquiring a skin area, which is an area of interest including personal information exposed from an image, is described. In Chapter 4, we describe the experimental results performed to measure the performance of the technique for acquiring a region of interest using illumination correction introduced in this paper. Finally, Chapter 5 explains the conclusion and future research directions.

## 2. Illumination Correction

In general, it is desirable to ensure sufficient illumination by arranging multiple high-power spot lights for high-speed cameras, but there is a disadvantage in that it is difficult to provide uniform intensity of illumination to the entire target object due to the characteristics of spot illumination. In other words, even if a lighting environment having a high illuminance is configured, a problem arises that it may be difficult to accurately confirm the shape of the target object since the actual photographing result is not uniform in illuminance. In recent years, due to the development of small image sensor elements of ultra-high-speed cameras, environmental dependence such as brightness and direction of lighting is getting better, but in order to obtain clearer images, an effective lighting device is also required according to the situation.

When an image is taken indoors using a high-speed camera, flickering occurs in the image. In fact, if you check the pixel values inside the ultra-high-speed image shot indoors, different illuminance values are applied even though they are almost the same scene every frame. The cause of this flickering phenomenon is related to the voltage and current specifications. Most countries typically use voltages and currents of 110V to 115V, 230V to 240V, and 50Hz or 60Hz. That is, since the electrical waves between 50 and 60 times per second are repeated, indoor incandescent lamps or LEDs flicker as much as the ratio of the waves. However, since the ultra-high-speed camera can capture about 10,000 frames per second or more, it can detect repeated light waves, so the flickering

phenomenon is naturally included in the image. Usually, when there is a flickering phenomenon in the image, the value of the lighting changes, so the color value representing the target object is also partially changed. Therefore, if the color value is not constant, there is a possibility that unwanted results may be derived by using an incorrect feature value when analyzing an image. Therefore, it is necessary to correct the uneven illuminance included in the image.

In this study, a frame blending technique is used to effectively compensate for such non-uniform luminance changes included in high-speed images [9]. In general, frame blending is an operation that generates a new image by multiplying the pixel values at the same location by a certain ratio in two images of the same size and then adding them, and is defined as Equation (1). In Equation (1),  $\alpha$  and  $\beta$  are weighting factors used to blend an image, and can have a value between 0 and 1, and the sum of the values of the two weighting factors [12-14] is 1. In this paper,  $\alpha$  and  $\beta$  are set equally to 0.5, which is commonly used. This weight can be adaptively adjusted through repetitive learning according to the indoor or outdoor situation located around the image being usually photographed. In addition,  $f_a(x, y)$  and  $f_b(x, y)$  denote two different input images, and  $f_r(x, y)$  denote a result image generated through frame blending.

$$f_r(x, y) = \alpha \times f_a(x, y) + \beta \times f_b(x, y) \quad (1)$$

$$\text{where } 0 \leq \alpha, \beta \leq 1, \alpha + \beta = 1$$

In this paper, first, the RGB color space of the input high-speed image is converted to the  $YC_bC_r$  color space [15-16], and frame blending is then applied only to the Y channel corresponding to the brightness value in the converted  $YC_bC_r$  color space to compensate for changes in lighting. In the  $YC_bC_r$  color space,  $C_b$  and  $C_r$  mean color values. Equation (2) shows an equation for converting RGB color space to  $YC_bC_r$  color space.

$$Y = 0.299 \times R + 0.587 \times G + 0.114 \times B \quad (2)$$

$$C_b = -0.16874 \times R - 0.33126 \times G + 0.5 \times B$$

$$C_r = 0.5 \times R - 0.41869 \times G - 0.08131 \times B$$

As a result, in this paper, the (R, G, B) color value of the input image is changed to the (Y,  $C_b$ ,  $C_r$ ) value using the color model conversion equation. Then, by substituting only the Y value corresponding to the illumination into Equation (1), a new Y' whose illumination of the input image is corrected is obtained. Finally, an image based on the original RGB color model can be obtained in reverse by applying the illumination-corrected (Y',  $C_b$ ,  $C_r$ ) values to Equation (3).

$$R = Y' + 1.402 \times C_r \quad (3)$$

$$G = Y' - 0.34414 \times C_b - 0.71414 \times C_r$$

$$B = Y' + 1.772 \times C_b$$

When looking at the resulting image of the frame blending used in this paper, it can be seen that the contrast is clearly displayed than before the frame blending was applied, and this can be visually confirmed through the histogram. That is, in the contrast histogram of the image to which the frame blending is applied, the contrast value is expressed non-uniformly as a whole due to the flickering phenomenon before the frame blending is applied. However, if frame blending is applied to properly correct the difference in lighting values between frames, since the lighting values in the image become relatively uniform, it can be confirmed that the histogram is normally displayed.

### 3. Acquisition of skin areas

In this paper, from the input image obtained in the previous step and corrected for non-uniform lighting using frame blending, the skin color distribution region, which is the region of interest representing the personal information of the exposed person, is extracted.

In general, the skin color feature provides very useful information for simple and effective detection of exposed body components such as human faces, necks, arms, and legs from an image. However, the task of accurately detecting the color area of the skin according to the surrounding environment in which the image is photographed, the fundamental difference in skin color existing between different races, noise, and color makeup is still one of the difficult problems to solve.

A search for related references suggests many existing algorithms for extracting human skin color. However, most of these methods detect skin color pixels from all input color images using a fixed single skin color distribution model created through learning for an image database of a certain size, so many false detections occur. In contrast, in this paper, a skin sample is obtained for each input image, a skin model is created, and then skin pixels are extracted, so that a more robust skin region can be extracted. In this paper, an eye is extracted from an input image, and a skin color distribution model is adaptively generated by automatically extracting the sample pixels around the extracted eye.

In this paper, the input color image is first changed to the  $YC_bC_r$  color model, which is widely known to be more suitable for skin pixel detection. The skin sample is then extracted and, through learning, an elliptical skin color model [17-18] that is standardized as shown in Equation (4) is generated. The generated skin model is then applied to the input image to separate human skin color pixels and non-skin color pixels.

$$\frac{(x - ec_x)^2}{a^2} + \frac{(y - ec_y)^2}{b^2} \leq 1 \quad (4)$$

In Equation (4),  $x$  and  $y$  represent the corresponding  $x$  and  $y$  coordinates of the two-dimensional elliptical equation.  $a$  and  $b$  mean the length of the major axis and minor axis of the ellipse. In addition,  $ec_x$  and  $ec_y$  are parameters for correcting the rotation error of the ellipse. The parameters used in this paper are empirically adjusted through repeated experiments.

In this paper, after detecting human skin pixels from the received test color image, we adopt an opening morphological operation in order to easily remove relatively small noise pixels that were erroneously detected [19-21]. Usually, the opening morphological operator is an operation that performs an erosion operation and then a

dilation operation. The opening operation  $B \circ S$  of the binary image  $B$  by the structuring element  $S$  is expressed as Equation (5).

$$B \circ S = (B \otimes S) \oplus S \quad (5)$$

In Equation (5),  $\oplus$  denotes the expansion operation, and  $\otimes$  denotes the erosion operation. In general, the expansion operation is performed by scanning a binary image with the structured element  $S$  as shown in Equation (6). When at least one element of  $S$  overlaps the object area  $B$  of the binary image, the pixel value located at the origin of the structured element is set to 1, otherwise it is assigned to 0.

$$B \oplus S = \begin{cases} 1 & \text{if } S \text{ overlaps } B \\ 0 & \text{otherwise} \end{cases} \quad (6)$$

On the other hand, the erosion operation scans the binary image with the structured element  $S$  as shown in Equation (7), and when all the pixels of  $S$  are included in the object area  $B$  of the binary image, the value of the pixel located at the origin of the structured element  $S$  is assigned to 1. In other cases, the pixel value is assigned to 0.

$$B \otimes S = \begin{cases} 1 & \text{if } S \in B \\ 0 & \text{otherwise} \end{cases} \quad (7)$$

In the opening operation, the target object becomes smaller due to the erosion operation, and the object is enlarged again by the expansion operation, so it may be considered that the same result as the original image will be produced, but this is not the case. In other words, the target object is reduced by the erosion operation and the convexly protruding area disappears. In addition, if there is noise, the noise disappears, but when the dilation operation is performed, the object becomes large in its original state, but the disappeared convex area does not appear convexly or the disappeared noise does not appear again.

Finally, after the opening morphological operation is applied, labeling for connecting adjacent pixels is applied to obtain the detected individual pixels as a skin area in units of separate areas.

#### 4. Results and Discussion

The computer used for the purpose of developing the algorithm proposed in this paper is composed of an Intel Core(TM) i7-6700 3.4 GHz CPU, 16 GB main memory, 256 GB SSD, and a Galaxy Geforce GTX 1080 Ti graphics card. In the system development computer, Microsoft Windows 10 was used as the operating system. In addition, Microsoft's Visual Studio 2017 was used as a development tool for the introduced lighting correction-based skin detection method. The OpenCV computer vision library was also used to efficiently implement the algorithm proposed in this study.

$$\Pi_{accuracy} = \frac{SKIN_{acquisition}}{SKIN_{total}} \times 100 \quad (\%) \quad (8)$$

In this study, the performance of the introduced method of acquiring skin pixels using illumination correction of high-speed input color images was quantitatively compared and measured in terms of accuracy. In this study, a measure such as Equation (8) described as the relative ratio of the number of skin regions correctly acquired in the received high-speed images and the number of skin regions originally included in all high-speed images was used. In Equation (8),  $SKIN_{acquisition}$  means the number of skin regions correctly acquired using the proposed algorithm.  $SKIN_{total}$  means the total number of skin areas included in the entire high-speed image used in the test. The quantitative accuracy equation used in this study is expressed as a percentage.

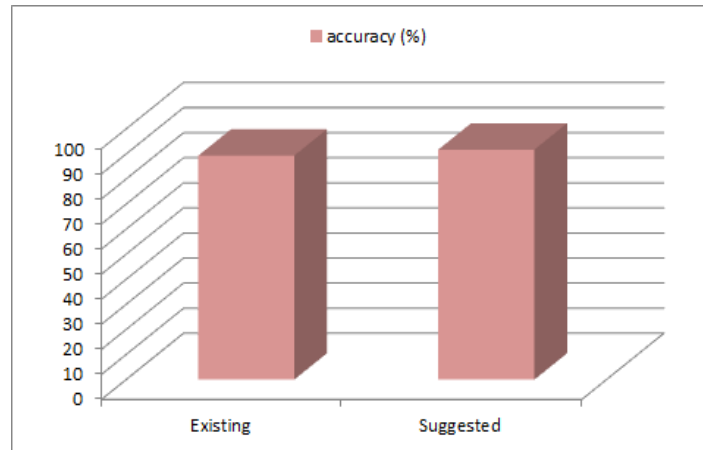


**Figure 2. Performance comparison**

Fig. 2 shows the performance of the method of acquiring a human skin area through illumination correction in terms of accuracy by comparing it with a bar graph. As can be seen in Fig. 2, the algorithm introduced in this paper uses the frame blending technique to more accurately obtain the area of interest, the exposed skin area.

In the conventional approach, the process of correcting irregular lighting in high-speed images was not normally performed. In addition, since a fixedly generated skin color distribution model is used, it is difficult to accurately extract skin pixels.

On the other hand, the algorithm introduced in this paper effectively corrects the uneven lighting effect reflected within the high-speed image through frame blending between successive images, and then acquires regions of interest, allowing it to obtain human skin color distribution regions more robustly than conventional approaches.

## 5. Conclusion

Ultra-high-speed cameras that can shoot images at very high speeds are becoming more and more common as their prices become relatively inexpensive in recent years, but related research has just entered the beginning stage. In particular, a high-speed camera that continuously accepts a large number of frames per second tends to reflect the lighting effect non-uniformly in a color image photographed according to changes in the surrounding environment. Therefore, there is a need for a study to effectively correct irregular illumination of ultra-high-speed images.

In this paper, we propose an algorithm that corrects lighting from ultra-high-speed color images that are

continuously input with a slight time interval, and robustly acquires the skin region, which is an area of interest, from the image corrected for lighting. In the proposed algorithm, non-uniform illumination is effectively corrected by using the frame blending technique from the ultra-fast color image received first. Then, using the elliptical color distribution model generated through learning, the exposed skin region, which is the region of interest, was robustly obtained from the color image corrected for illumination. In the experimental results, it was described that the algorithm introduced in this study corrects the lighting from the input high-speed color image, and then robustly acquires the skin color region from the image data that the lighting is corrected.

In the future, we plan to reinforce the stability of the algorithms established so far by repeatedly applying the method of acquiring the region of interest through correction of lighting introduced in this paper to more diverse types of test images. In addition, the proposed method will be tested not only in the general lighting environment during the day, but also in the harsher environments such as dawn, evening, and dense fog to increase the scalability of the system.

## 6. Acknowledgment

This work was supported by the National Research Foundation of Korea (NRF) grant funded by the Korea government (MSIT) (2019R1F1A1056475)

## 7. References

1. Javh J, Slavic J, Boltezar M. High frequency modal identification on noisy high-speed camera data. *Mechanical Systems and Signal Processing*. 2018 Jan; 98:344-351. DOI: <https://doi.org/10.1016/j.ymssp.2017.05.008>
2. Jung W, Hurth C, Zenhausern F. Real-time monitoring of viscosity changes triggered by chemical reactions using a high-speed imaging method. *Sensing and Bio-Sensing Research*. 2015 Sep;5:8-12. DOI: <https://doi.org/10.1016/j.sbsr.2015.05.003>
3. Ma Z, Han M, Li Y, Gao H, Lu E, Chandio FA, Ma K. Motion of cereal particles on variable-amplitude sieve as determined by high-speed image analysis. *Computers and Electronics in Agriculture*. 2020 Jul;174:1-9. DOI: <https://doi.org/10.1016/j.compag.2020.105465>
4. Jung W, Hurth C, Zenhausern F. Real-time monitoring of viscosity changes triggered by chemical reactions using a high-speed imaging method. *Sensing and Bio-Sensing Research*. 2015 Sep;5:8-12. DOI: <https://doi.org/10.1016/j.sbsr.2015.05.003>
5. Yap MH, Goyal M, Osman F, Marti R, Denton E, Juette A, Zwiggelaar R. Breast ultrasound region of interest detection and lesion localisation. *Artificial Intelligence in Medicine*. 2020 Jul;107:1-8. DOI: <https://doi.org/10.1016/j.artmed.2020.101880>
6. Hu CH, Yu J, Wu F, Zhang Y, Jing XY, Lu XB, Liu P. Face illumination recovery for the deep learning feature under severe illumination variations. *Pattern Recognition*. 2021 Mar;111:1-13. DOI: <https://doi.org/10.1016/j.patcog.2020.107724>
7. Liao B, Hu J, Gilmore RO. Optical flow estimation combining with illumination adjustment and edge refinement in livestock UAV videos. *Computers and Electronics in Agriculture*. 2020 Dec;180:1-12. DOI: <https://doi.org/10.1016/j.compag.2020.105910>
8. Saeed U, Masood K, Dawood H. Illumination normalization techniques for makeup-invariant face recognition. *Computers and Electrical Engineering*. 2020 Nov;89:1-14. DOI: <https://doi.org/10.1016/j.compeleceng.2020.106921>



9. Goswami S, Singh SK. A simple deep learning-based image illumination correction method for paintings. *Pattern Recognition Letters*. 2020 Aug;138:392-396. DOI: <https://doi.org/10.1016/j.patrec.2020.08.013>
10. Mishra P, Lohumi S, Khand HA, Nordon A. Close-range hyperspectral imaging of whole plants for digital phenotyping: recent applications and illumination correction approaches. *Computers and Electronics in Agriculture*. 2020 Sep;178:1-11. DOI: <https://doi.org/10.1016/j.compag.2020.105780>
11. Zhu Z, Liu H, Lu J, Hu SM. A metric for video blending quality assessment. *IEEE Transactions on Image Processing*. 2019 Nov;29:3014-3022. DOI: <https://doi.org/10.1109/TIP.2019.2955294>
12. Yu Y, Yang T, Chen H, Lamare RCD, Li Y. Sparsity-aware SSAF algorithm with individual weighting factors: performance analysis and improvements in acoustic echo cancellation. *Signal Processing*. 2020 Sep;178:1-16. DOI: <https://doi.org/10.1016/j.sigpro.2020.107806>
13. Yu Y, Zhao H. Novel sign subband adaptive filter algorithms with individual weighting factors. *Signal Processing*. 2016 May;122:14-23. DOI: <https://doi.org/10.1016/j.sigpro.2015.11.007>
14. Saqib N, Siddiqi MT. Determination of weighting factors for safety performance indicators in NPPs. *Safety Science*. 2016 Apr;84:245-249. DOI: <https://doi.org/10.1016/j.ssci.2015.12.002>
15. Muhammad K, Sajjad M, Mehmood I, Rho S, Baik SW. Image steganography using uncorrelated color space and its application for security of visual contents in online social networks. *Future Generation Computer Systems*. 2016 Nov;86:951-960. DOI: <https://doi.org/10.1016/j.future.2016.11.029>
16. Zhu SY, He ZY, Chen C, Liu SC, Zhou J, Guo Y, Zeng B. High-quality color image compression by quantization crossing color spaces. *IEEE Transactions on Circuits and Systems for Video Technology*. May 2019;29(5):1474-1487. DOI: 10.1109/TCSVT.2018.2841642
17. Hsu RL, Abdel-Mottaleb M, Jain AK. Face detection in color images. *IEEE Transactions on Pattern Analysis and Machine Intelligence*. 2002 May;24(5):696-706. DOI: <https://doi.org/10.1109/34.1000242>
18. Chakraborty BK, Bhuyan MK, Kumar S. Combining image and global pixel distribution model for skin colour segmentation. *Pattern Recognition Letters*. 2017 Mar;88:33-40. DOI: <https://doi.org/10.1016/j.patrec.2017.01.005>
19. Su R, Sun C, Zhang C, Pham TD. A new method for linear feature and junction enhancement in 2D images based on morphological operation, oriented anisotropic gaussian function and hessian information. *Pattern Recognition*. 2014 Oct;47(10):3193-3208. DOI: <https://doi.org/10.1016/j.patcog.2014.04.024>
20. Hamuda E, Ginley BM, Glavin M, Jones E. Automatic crop detection under field conditions using the HSV colour space and morphological operations. *Computers and Electronics in Agriculture*. 2017 Feb;133:97-107. DOI: <https://doi.org/10.1016/j.compag.2016.11.021>
21. Zhang Y, Ji TY, Li MS, Wu QH. Identification of power disturbances using generalized morphological open-closing and close-opening undecimated wavelet. *IEEE Transactions on Industrial Electronics*. 2016 Apr;63(4):2330-2339. DOI: 10.1109/TIE.2015.2499728